8684 *Biochemistry* **2009,** *48,* 8684–8691
DOI: 10.1021/bi900868e

BIOCHEMISTRY
including biophysical chemistry & molecular biology
Article

A C-Terminal Lobe of the β Subunit of Na,K-ATPase and H,K-ATPase Resembles Cell Adhesion Molecules†

Elizabeta Bab-Dinitz,‡ Shira Albeck,§ Yoav Peleg,§ Vlad Brumfeld,∥ Kay E. Gottschalk,⊥ and Steven J. D. Karlish*,‡

‡*Department of Biological Chemistry and* §*Department of Structural Biology and* ∥*Department of Plant Sciences, Weizmann Institute of Science, Rehovoth 76100, Israel, and* ⊥*Department of Applied Physics, Ludwig-Maximilians Universität, 80799 München, Germany*

Received May 22, 2009; Revised Manuscript Received August 13, 2009

ABSTRACT: The β subunit of Na,K-ATPase is required for stabilization and maturation of the catalytic α subunits and is also involved in cell adhesion and establishing epithelial cell polarity. However, the mechanism of cell adhesion effects and protein partners of β are unknown. We have applied fold recognition methods to predict that a C-terminal domain of the β subunits of Na,K-ATPase and H,K-ATPase has an immunoglobulin-like fold, which resembles cell adhesion molecules. Comparison of the predicted C-terminal domain with a recently published structure of shark rectal gland Na,K-ATPase at 2.4 Å in which α, β, and FXYD subunits were resolved confirms that the β subunit ectodomain contains an immunoglobulin-like structure. Expression in *Escherichia coli* of a sequence corresponding to the C-terminal domain, followed by its purification, refolding, and circular dichroism analysis, shows that the domain is independently stable with prominent β sheet secondary structure, as predicted. Proteolytic digestion of the purified detergent-soluble recombinant Na,K-ATPase (α1β1) is also indicative of a stable C-terminal domain of β in the native complex. The major conclusion of this work is consistent with prior evidence for a role of the β subunit in cell−cell adhesion, and it attributes that function largely to the C-terminal lobe of the β ectodomain. In the light of these findings, we discuss its role in cell adhesion and recognition of the β subunits of Na,K-ATPase, including potential protein partners.

The Na,K-ATPase (Na,K-pump) belongs to the P-type ATPase family of cation pumps. The Na,K-ATPase and related H,K-ATPase consist of α and β subunits. The α subunits transport the cations and couple active transport to hydrolysis of ATP. The β subunit is necessary for the proper folding in the endoplasmic reticulum, for routing and insertion into the plasma membrane, and for structural and functional stabilization of the mature α subunit. In addition, the β subunit influences the K activation kinetics and may be required for stabilization of the K-transporting conformations of mature Na,K-ATPase and H,K-ATPase (*1*, *2*). Three isoforms of β (β1−β3) of Na,K-ATPase are known.

Recently, an additional role of the β1 subunit of Na,K-ATPase in epithelial cell−cell contact has been described. β1 has been shown to be localized at the cell−cell contacts in polarized epithelial cells, from the initial steps of their formation, colocalized with E-cadherin at the sites of Adherens Junctions (AJ),[1] and play an important role in epithelial cell polarization (*3*−*5*). Overexpression of the β1 isoform in Maloney sarcoma virus-transformed Madin Darby canine kidney cells has been shown to reduce cell motility (*6*). An antibody against the β1 ectodomain specifically inhibits cell−cell contacts (*5*, *7*). Normal glycosylation of the β1 subunit also appears to play an important role in cell−cell contacts (*5*, *8*). On the basis of this work, it has been suggested that the β1 subunit mediates cell−cell contacts directly or via interactions with other proteins (*5*, *9*). The β2 isoform has long been known to act as a cell adhesion molecule between astrocytes and neurons in brain (*10*), showing that this function of β is not restricted to epithelia. However, the mechanism of β-mediated cell adhesion or specific protein partners of β are not known.

The β subunits of Na,K-ATPase and H,K-ATPase are type II membrane glycoproteins with a single transmembrane segment, a short cytoplasmic tail (N-terminus), and a large extracellular domain (ectodomain), with three conserved S−S bridges and conserved glycosylation sites (*1*). Interactions between α and β subunits are mediated by the transmembrane segments, ectodomains, and cytoplasmic parts (*1*). However, the ectodomain of the β subunit suffices for assembly with α (*11*). The SYGQ sequence in the extracellular loop of α, L7/8, is a key region of interaction with β (*12*).

The structure at 3.5 Å of the native renal Na,K-ATPase, containing α, β, and γ (FXYD2) subunits, was published recently (PDB entry 3B8E) (*13*). The α subunit, the transmembrane helix, and a short extracellular fragment of β and transmembrane segment of the γ subunit were resolved. The ectodomain of β was not resolved. The β subunits of Na,K-ATPase and H,K-ATPase have no closely related homologues with known structure. Therefore, homology modeling was precluded. In this situation, fold recognition structure prediction methods, which search for distant homology between a target protein of unknown structure

†This work was supported by a Grant 433/09 from the Israel Science Foundatation and by the Mauerberger Foundation (Cape Town, South Africa). This work was conducted in collaboration with the Israel Structural Proteomics Center (ISPC), supported by The Israel Ministry of Science, Culture, and Sport, the Divadol Foundation, the Neuman Foundation, and the European Commission Sixth Framework Research and Technological Development Program 'SPINE2-COMPLEXES' Project (Contract 031220).

*To whom correspondence should be addressed. Telephone: 972 8 934 2278. Fax: 972 8 934 4118. E-mail: Steven.Karlish@weizmann.ac.il.

[1]Abbreviations: AJ, Adherens Junctions; $C_{12}E_8$, octaethylene glycol monodecyl ether; HPLC, high-performance liquid chromatography; ED, electron density; CD, circular dichroism; CAM, cell adhesion molecules; PDB, Protein Data Bank.

 Published on Web 08/20/2009

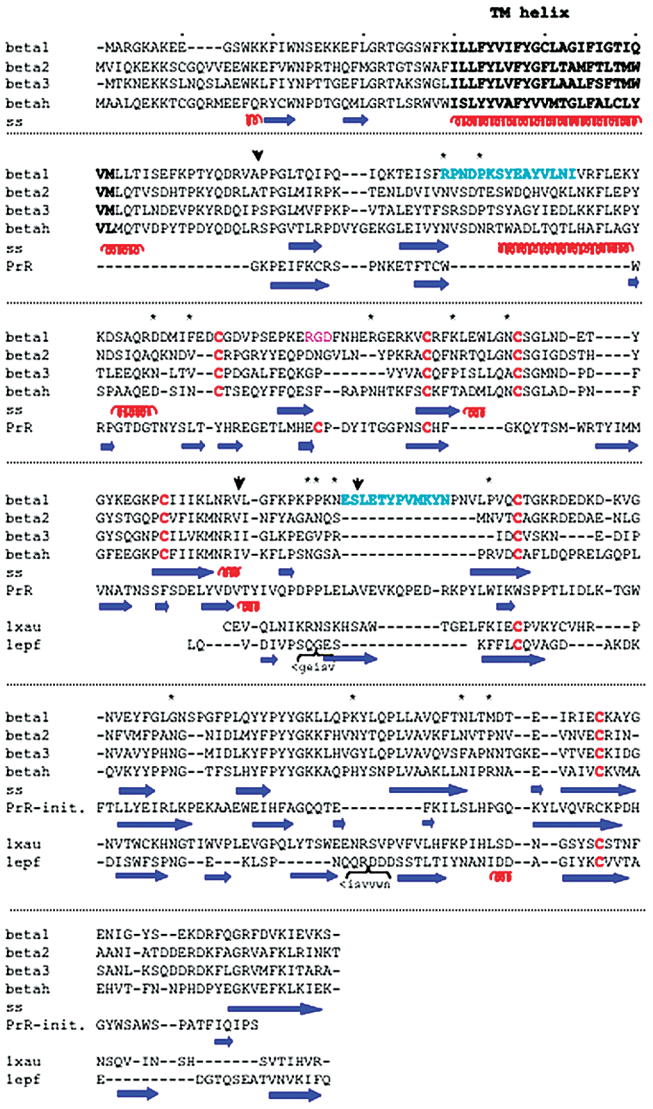

FIGURE 1: Sequence alignment between the β subunit of Na,K-ATPase and H,K-ATPase and the structural templates predicted by fold recognition methods. Human $\beta1-\beta3$ of Na,K-ATPase and the β subunit of H,K-ATPase were aligned using ClustalW. Positions of identical amino acids in the four sequences are shaded in gray. The cysteine residues participating in the S−S bridge formation are bold and colored red. The asparagines of the predicted N-terminal glycosylation sites are denoted with asterisks. The sequence of the transmembrane helix is bold. Secondary structure prediction for the β subunit ectodomain from the Bioinfo.pl meta-server is shown below the sequences of the isoforms (blue arrows for β strand and red coils for α helix). The sequences of the template structures used for the generation of the initial model of Na,K-ATPase β [1bp3 of the prolactin receptor (PrP)] and models of the C-terminal domain of Na,K-ATPase $\beta1$ and $\beta2$ [1xau (B- and T-lymphocyte attenuator (BTLA)] and of H,K-ATPase β {1epf [the N-terminal domains of neural cell adhesion molecule (NCAM)]} are shown with the alignment predicted by the 3D-Jury meta-server. The cysteines of the template structures corresponding to those of the β subunits are bold and colored red. Arrows indicate the beginning and the end of the modeled parts of the $\beta1$ isoform. The RGD motif in $\beta1$ is colored pink. Sequences colored cyan were estimated to include residues in contact with the α subunit (*36*). Two sequence boxes indicate insertions in the template structures relative to the β sequence according to the predicted alignment.

and proteins with known structure, can be invaluable (*14*, *15*). We have used the 3D-Jury fold recognition meta-server to predict a putative fold of the β subunit ectodomain. In general, meta-servers for fold prediction and distant homology detection outperform individual autonomous servers, and 3D-Jury is one of the best performing meta-servers (*15*). The fold of a C-terminal lobe of the β subunits of Na,K-ATPase and H,K-ATPase predicted by the 3D-Jury meta-server resembles the fold of cell−cell adhesion and cell recognition molecules. We have also tested and found support for this concept by two independent biochemical approaches. At the time this paper was being prepared, the structure of the β subunit ectodomain was not known. In the meantime, a structure of shark rectal gland Na,K-ATPase at 2.4 Å has been published with details of the structure of the β subunit ectodomain (*16*). The predictions of the modeling and the actual structure are compared in Discussion. This confirms the existence of an immunoglubulin-like fold in the C-terminal half of the β subunit.

MATERIALS AND METHODS

Modeling. Sequences of human β isoforms of the Na,K-ATPase (Swiss-Prot accession numbers P05026, P14415, and P54709) and H,K-ATPase β (Swiss-Prot accession number P51164), whole or only their ectodomains, were submitted to the 3D-Jury Bioinfo.pl structure prediction meta-server (www.bioinfo.pl/meta). The models in Figures 3 and 4 were based on one of the high-scoring structural templates for each submitted query (1xau for $\beta1$ and $\beta2$ and 1epf for βHK). The alignment from the Bioinfo.pl meta-server (see Figure 1) was used to build the models using SWISS-MODEL or MODELER. Ramachandran plots obtained using PROCHECK showed that nearly all side chains were in allowed positions (for example, for $\beta1$ 69.9% in most favored regions, 25.8% in allowed regions, 4.3% in generously allowed regions, and 0% in disallowed regions, accounting for 100% of non-glycine and non-proline residues). The model for the C-terminal lobe of $\beta1$ was manually fitted to the 11 Å electron density map of the Na,K-ATPase (*17*), and the C-terminal lobe of H,K-ATPase was fitted to a 6.5 Å electron density map (*18*), using the Chimera UCSF program.

Expression, Purification, and Refolding. C-Terminal fragments of human $\beta1$ corresponding to resides 184−302, 186−302, and 191−302, were expressed in the *Escherichia coli* BL21(DE3) strain using the pET28-TEVH vector as described previously (*19*). Bacteria were grown at 37 °C in LB medium containing 30 μg/mL kanamycin. At an A_{600} of 0.7, protein expression was induced by the addition of 0.5 mM IPTG. After 3 h, the cells were harvested and resuspended in lysis buffer containing 50 mM Tris (pH 7.5), 150 mM NaCl, 1 mM EDTA, 100 μg/mL lysozyme, and 0.5 mM PMSF. The overexpressed protein, found in the insoluble fraction of the cell lysate, was separated by centrifugation. The inclusion bodies were washed several times with 50 mM Tris (pH 7.5), 100 mM NaCl, and 0.5% Triton X-100 followed by a final wash without Triton X-100. Washed inclusion bodies were dissolved in 8 M urea or 6 M guanidine HCl and incubated overnight at 4 °C. The denatured protein was purified using TALON Co^{2+} beads and eluted at a concentration of 0.1 mg/mL with 150 mM imidazole. For refolding, the denatured purified protein was diluted 1:10 (v:v) dropwise into a buffer containing 50 mM Tris (pH 8.6), 0.4 M arginine, and 0.5 mM EDTA under vigorous stirring at 20 °C and incubated at 4 °C for at least 20 h with gentle stirring. The protein was filtered using Millipore 0.22 μ filters and concentrated using Millipore Amicon Ultra centrifugal filter devices. The concentrated protein was dialyzed twice against 40 mM Tris (pH 8.5); insoluble protein was removed by centrifugation (30 min at 16000*g*), and the supernatant

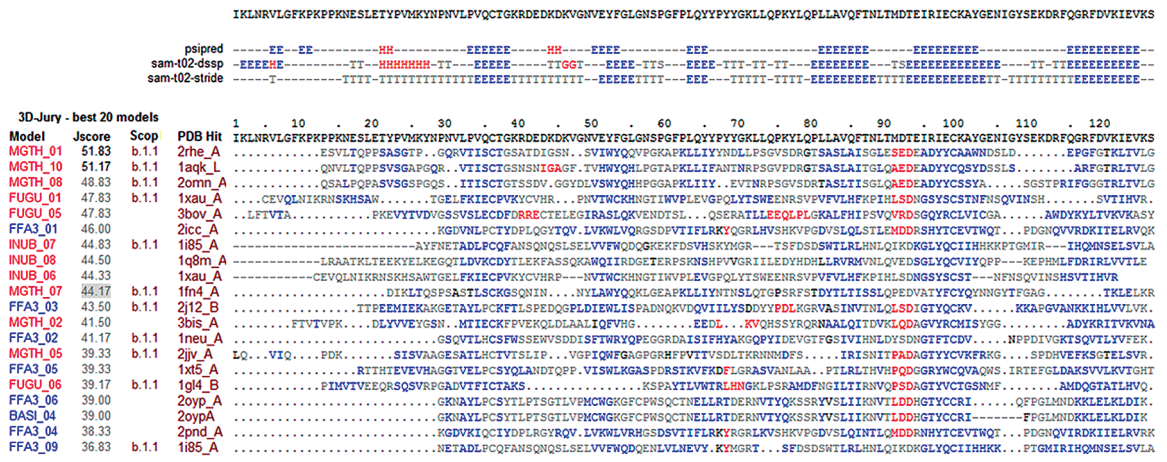

FIGURE 2: Secondary structure alignment of the C-terminal domain of the Na,K-ATPase β1 subunit and template structures. Top line: sequence of human β1 from residue Ile177. Lines 2−4: psipred, sam-t02-dssp, sam-t02-stride; secondary structure predictions for β1: E (blue) for β strand, H (red) for α helix, T (gray) for unordered. Lines 5−22: 3D-Jury predictions; blue for β strand, red for α helix, gray for unordered. Model: model ID (specific server abbreviation with the number of the 10 best models). Jscore: 3D-Jury scores for different models in ascending order. Scop: SCOP classification of the template structure. b.1.1-Immunoglobulin Superfamily belonging to the immunoglobulin-like β sandwich fold. PDB Hit: template structure name from the PDB.

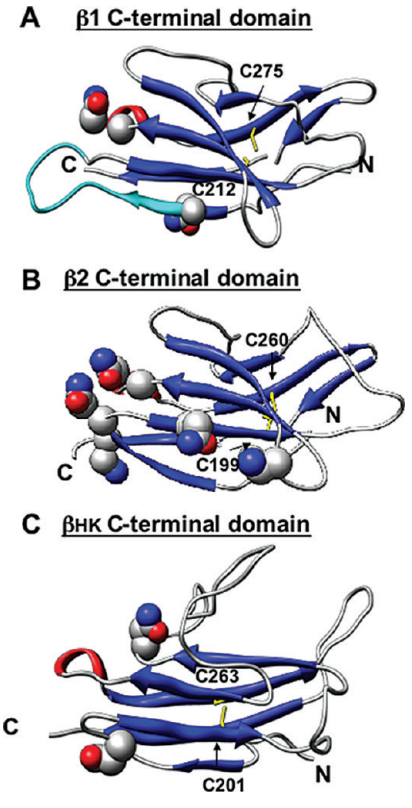

FIGURE 3: Models of the ectodomains of β1, β2, and βHK. (A and B) Models for the C-terminal lobes of β1 and β2 based on template 1xau [B- and T-lymphocyte attenuator (BTLA)]. (C) Model of βHK based on 1epf [the N-terminal domains of neural cell adhesion molecule (NCAM)]. β strands are colored blue, loops gray, and cysteines yellow; asparagine residues of predicted N-glycosylation sites are depicted as spheres. The segment thought to include residues close to α (*36*) is colored cyan. N- and C-termini are indicated. Cysteines are numbered.

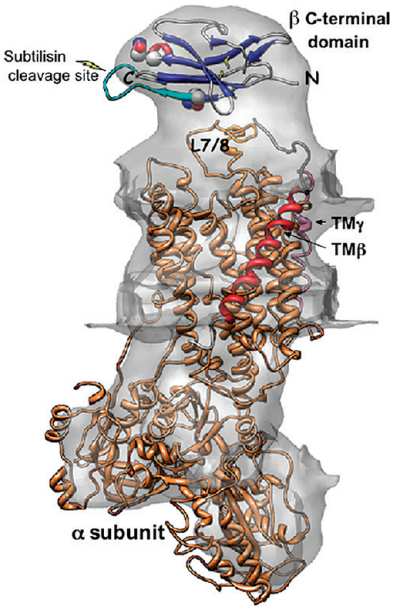

FIGURE 4: Model of the C-terminal lobe of the β1 ectodomain fitted into the 11 Å resolution electron density map of the Na,K-ATPase β1 model colored as in Figure 3A. In the 3B8E structure, the α subunit is colored wheat, the transmembrane segment of β red, and the extracellular fragment of β dark gray. The transmembrane segment of γ is colored pink. The subtilisin cleavage site is indicated (see Figure 7).

was used for further analysis. Size exclusion chromatography was conducted using a Superdex 200 (Healthcare 10/300 GL) column. The running buffer contained 40 mM Tris (pH 8.5) and 150 mM NaCl. The identity of the purified protein was confirmed by MALDI-TOF mass spectrometry.

Circular Dichroism Analysis. CD measurements were performed in a Cirascan circular dichroism spectrophotometer (Applied Photonics). The CD spectra of the refolded protein, at 0.4 mg/mL, were recorded in a 0.1 mm path length fused silica cuvette. Spectra were averages from 10 runs, each measured between 190 and 260 nm with a time constant of 0.5 s/point and a spacing of 0.3 nm. Secondary structural estimations were performed with an in-house fitting algorithm (*20*) as well as with the Java Applet K2D2 (*21*).

Proteolytic Cleavage. Human α1β1 was expressed in *Pichia pastoris*, and the detergent-soluble, purified, and EndoH-deglycosylated α1β1 complex was prepared as described previously (*22*). The purified protein was used for proteolysis

(10 min at 37 °C) with subtilisin, chymotrypsin, thermolysin, and trypsin at a 1:1 (w:w) ratio (10−20 μg of the protein) in a buffer containing Tris-HCl (pH 8.0) and 1 mM $CaCl_2$. Proteolysis was stopped with 10% (v:v) TCA, and the suspensions were centrifuged for 10 min at 16000*g* and washed twice with cold acetone. The final pellet was resuspended in 1× SDS−PAGE loading buffer. For Coomassie blue staining of gels, the whole pellet from 10 to 20 μg, and for immunoblots from 1 to 2 μg, was loaded per lane. For N-terminal sequencing, proteolytic fragments from 20 μg of protein were separated via 12% SDS−PAGE, transferred to a PVDF membrane, and stained with Coomassie blue.

RESULTS

Models of a C-Terminal Domain of β1, β2, and βHK. The sequences of the three human Na,K-ATPase β subunit isoforms, and the β subunit of H,K-ATPase (βHK), or the ectodomains, were submitted to the 3D-Jury meta-server (*14*), resulting in a very similar secondary structure prediction for the three Na,K-ATPase β isoforms and H,K-ATPase β (see Figure 1). The majority of results for the β1 ectodomain (18 of 20) were based on templates with the immunoglobulin fold, with prominent β strand secondary structure (Jscore ≤ 32, a relatively low score). As seen in Figure 1, there is a reasonably good alignment with β strand segments of the templates. One significant difference is that β is predicted to have a long α helical segment (S96−D118), while the templates are almost devoid of α helices. Most of the initial models, of the whole ectodomain, were based on the extracellular domains of cytokine and peptide hormone receptors, such as the prolactin receptor (1bp3), consisting of two lobes connected by a flexible linker, and were relatively low-scoring. However, it is significant that although eight predicted templates covered the whole ectodomain, eight models covered only the C-terminal half of the ectodomain (approximately from Ile177 to Ser302), predicting this segment to have an immunoglobulin-like fold.

The initial prediction that the ectodomain consists of two domains led us to submit the sequences of two hypothetical domains separately to the 3D-Jury meta-server (i.e., Val71−Leu179 and Ile177−Ser302). If these sequences correspond to two independent lobes, this approach should lead to improved scores of individual lobes and, in any case, test the initial hypothesis. No high-scoring results of the N-terminal half of the ectodomain (up to Leu179) were obtained, implying that this half of the ectodomain probably does not have an independent structure. By contrast, the Jscores for the predicted C-terminal lobe (greater than or equal to that of Ile177−Ser302) were much higher (≤52) than for the whole ectodomain (Jscore ≤ 32). As described in refs *15* and *23*, experience shows that a Jscore of > 50 is highly significant, predicting an overall fold that is structurally similar to the corresponding experimental structures in more than 90% of the cases. A remarkable alignment of the predicted β strand segments of this part of β1 and of the β strand segments of the templates was apparent (see Figure 1 for template 1xau and Figure 2 for the 20 best templates for β1, with Jscores). These results lead to the model in Figure 3A. Interestingly, all the templates belong to structural families having the immunoglobulin-like V-set or I-set fold, and the majority are cell−cell recognition or adhesion molecules. The template structures have two cysteines forming an S−S bridge, which are aligned with the third conserved pair of cysteines of the β1 isoform known to form an S−S bridge (Figures 1 and 2). Like the β ectodomain, the templates are ectodomains of single transmembrane segment proteins.

Homologous sequences of the β2 isoform of Na,K-ATPase and the H,K-ATPase β subunit produced quite similar results (Jscore for β2 ≤ 52, and Jscore for βHK ≤ 58) (see Figure 3B,C). The alignment of the secondary structure of the C-terminal lobe of the β2 and βHK ectodmain with the templates is quite similar to that for β1, and again, nearly all templates are cell recognition or adhesion molecules.

The model for the C-terminal lobe of β1, based on the template (1xau), was manually fitted to an 11 Å resolution electron density (ED) map of Na,K-ATPase (*17*) (Figure 4). As a first step, the published structure [3B8E (*13*)] was fitted to the ED map and the extra density was assumed to correspond to the β ectodomain. The question was whether the dimensions and orientation of the model for the C-terminal lobe of β are compatible with the ED map. As seen in Figure 4, the model fits nicely into the electron density map, at a position corresponding to the most outer region of the ectodomain. This position was assumed to be correct as it leaves space for the N-terminal segment of the ectodomain in the unassigned electron density, closer to the transmembrane segment of β. To choose an optimal orientation, the molecule was rotated until the minimal mass protruded from the electron density map. When the molecule was placed using this criterion, the two N-glycosylation sites face away from the α subunit, toward the extracellular medium. This provides some independent support that the chosen orientation is optimal.

Biochemical Tests of the Model. (*i*) *Expression, Purification, Refolding, and CD Analysis of the C-Terminal Lobe of β1.* The model in Figures 3 and 4 predicts that the C-terminal lobe is an independently stable globular domain, containing a high proportion of β strand secondary structure. We have tested this by expressing and purifying the protein and analyzing its secondary structure. Since the exact boundaries were not known, we selected three segments (residues 184−302, 186−302, and 191−302) of human β1 for expression in *E. coli* as His-tagged fusion proteins (see Materials and Methods). Figure 5A shows strong expression of residues 184−302 and 191−302 in the induced compared to the control bacteria (strong expression of residues 186−302 was also observed but is not shown). The expressed proteins were found only in insoluble inclusion bodies, and thus, it was necessary to dissolve them in 8 M urea or 6 M guanidine, purify them, and then refold the protein (see Materials and Methods). The electrophoretic mobility of fragment 191−302 in the absence of β-mercaptoethanol showed no signs of protein dimerization or aggregates, and the mobility was slightly faster, than in the presence of β-mercaptoethanol (not shown). This suggested that nonspecific aggregation via intermolecular S−S bond formation is negligible, and that the single predicted intramolecular S−S bridge is formed. Therefore, subsequent purification and refolding were conducted in the absence of reducing agents. Figure 5B shows a gel with the soluble purified and refolded 191−302 fragment (PR) next to unpurified protein in inclusion bodies (IB). Between 10 and 20% of the initial insoluble material was retrieved as purified refolded protein.

The refolded protein was applied to a size exclusion column and was eluted at a volume corresponding to the monomer (with a calculated mass of 13−15 kDa in different runs) (Figure 6A). The secondary structure was then analyzed by CD spectroscopy, which shows a weak negative signal at ~212 nm (Figure 6B). This feature disappeared when the protein was heated at 95 °C in the

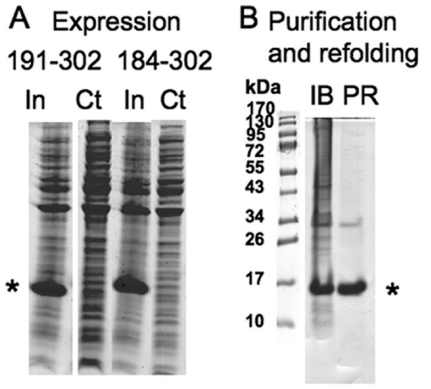

FIGURE 5: Expression, purification, and refolding of the C-terminal domain of β1. (A) Expression of recombinant fragments 191−302 and 184−302 in *E. coli* BL21(DE3) cells. Whole cell lysates uninduced (Ct) and after induction with IPTG for 6 h at 30 °C (In). (B) Fragment 191−302 in inclusion bodies (IB) and the soluble, metal affinity chromatography purified and refolded protein (PR): IB, 32 μg of protein; PR, 12 μg of protein.

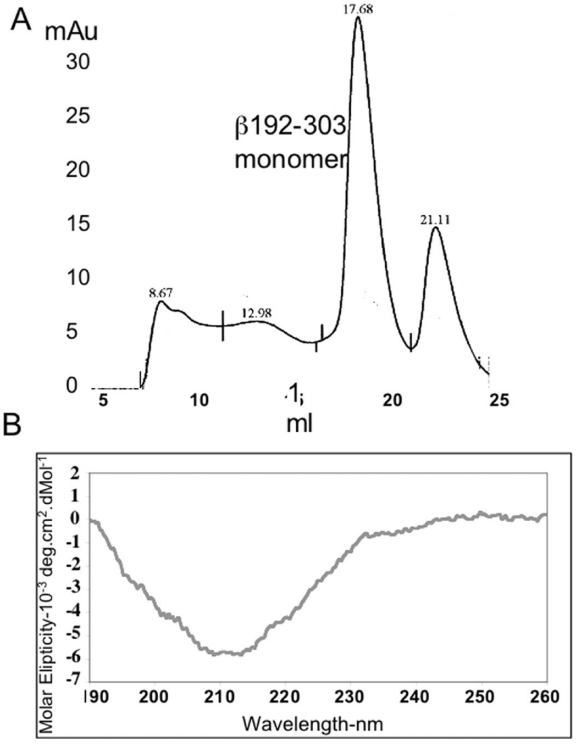

FIGURE 6: Size exclusion chromatography and CD spectroscopy of purified refolded fragment 191−302. (A) Size exclusion HPLC was performed in a running buffer containing 40 mM Tris (pH 8.5) and 150 mM NaCl (170 μg of protein). (B) Smoothed CD spectra obtained using 50 μL of 0.4 mg/mL protein in 40 mM Tris-HCl (pH 8.5).

presence of dithiothreitol (not shown). Calculations of secondary structure by two different programs predicted 41−45% β strand and 51−55% disordered protein. This agrees with 35% β strand (and the rest disordered) predicted by the model of β1 in Figure 3A. Overall, the measured properties of the purified C-terminal lobe suggest that the fragment is correctly folded and are compatible with the proposed model.

(*ii*) *Proteolytic Cleavage of* β *in the* $\alpha 1\beta 1$ *Complex*. If the C-terminal lobe is an independent domain within the intact $\alpha\beta$ complex, it should be resistant to proteolytic cleavage, except at selective positions, accessible from the medium. The data in Figure 7 present proteolytic cleavages of the purified

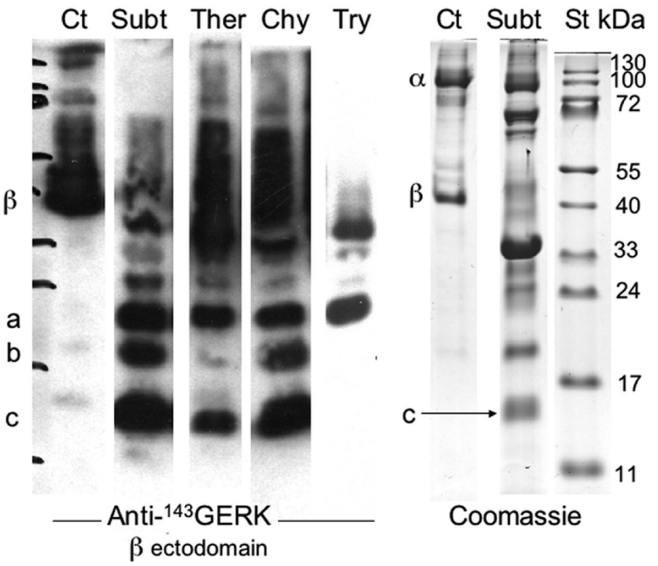

FIGURE 7: Proteolytic cleavage of β1 in the purified $\alpha 1\beta 1$ complex. (A) Proteolysis with protease [purified human $\alpha 1\beta 1$ complex, 1:1, w-w], subtilisin (Subt), thermolysin (Ther), chymotrypsin (Chy), and trypsin (Try). Immunoblots were performed using anti-^{143}GERK (anti-β1). (B) Coomassie blue stain of untreated control $\alpha 1\beta 1$ complex (Ct) and subtilsin (Subt)-cleaved $\alpha 1\beta 1$ complex.

detergent-soluble and deglycosylated human $\alpha 1\beta 1$ complex (*22*), using subtilisin, thermolysin, chymotrypsin, and trypsin. Very high concentrations of subtilsin, thermolysin, and chymotrypsin produced only three fragments, a, b, and c with apparent masses of 20.3, 17.5, and 13.5 kDa, respectively (Figure 7A). The 13.5 kDa subtilisin fragment was produced in sufficient quantity, and separated from other fragments, for N-terminal sequencing, which identified Tyr203 (YNPNVL sequence) (Figure 7B). The major subtilisin cleavage site is located in an accessible loop near the beginning of the C-terminal lobe (depicted in Figure 4). Thermolysin and chymotrypsin presumably also cut at or near the same site. The 20.3 and 17.3 kDa subtilisin fragments were not produced in sufficient quantities for sequencing. Trypsin, at a very high concentration, produced two fragments with apparent masses of 21.4 and 33 kDa (Figure 7A). N-Terminal sequencing was not possible due to overlap with fragments of the α subunit. However, on the basis of previous work on renal Na,K-ATPase, the N-terminus of the 21.4 kDa fragment can be assigned as at or near G143 in the N-terminal half of the ectodomain (with a predicted mass for G143−Ser303 of 18.6 kDa) (*24*).The 33 kDa tryptic fragment is cut near the cytoplasmic N-terminus of β. Overall, the proteolytic cleavages show that the ectodomain of β in the whole $\alpha\beta$ complex is a compact structure with few accessible cleavable bonds.

DISCUSSION

This work presents a structure prediction for the C-terminal part of the β subunit ectodomain (β1, β2 and βHK), tests of the predicted fold by independent expression and analysis of the modeled fragment, and hypotheses about possible protein−protein interactions. As mentioned in the introductory section, since this work was written an atomic-resolution structure of the β subunit ectodomain has been published (*16*). The newly published structure of the shark Na,K-ATPase at 2.4 Å includes the resolved structure of the β ectodomain, which appears to be a singe compact domain having a unique fold. The ectodomain indeed contains an immunoglobulin-like structure similar to that

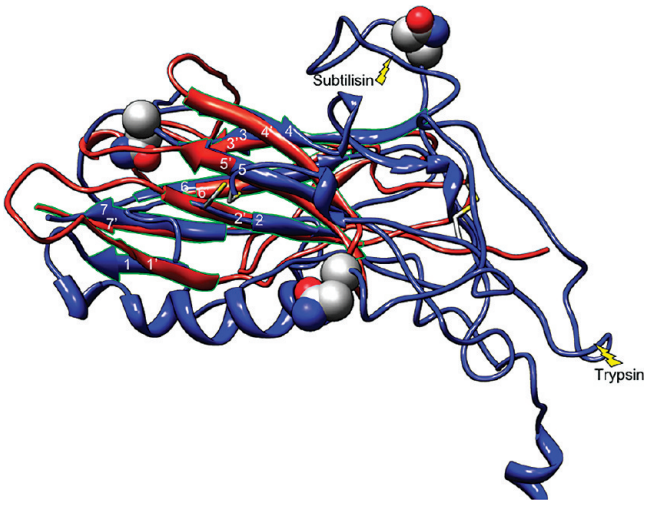

FIGURE 8: Comparison of the predicted fold of the C-terminal domain and the actual structure of the β subunit ectodomain: red for the model and blue for the β subunit structure (2ZXE_B). Positions of tryptic (*24*) and subtilisin cleavage sites and glycosylation sites are indicated.

predicted by the fold recognition methods. Moreover, several of the best template structures, predicted by the fold recognition meta-server, appear within the results of the Dali server (*25*), which predicts similarity to actual structures, in this case the β subunit (2zxe_B). These include 1neu (neural membrane adhesion molecule P0), 1xau [B- and T-lymphocyte attenuator (BTLA)], 1pko [myelin oligodendricyte glycoprotein (MOG)], 1aqk (immunoglobulin FAB), 2rhe [λ-type Bence-Jones protein (RHE)], and 1fn4 (immunoglobulin FAB).

Structural superimposition between the model of the human β1 C-terminal lobe and the structure of the shark β1 ectodomain is shown in Figure 8. As can be seen, the overall fold of the model for the C-terminal part of the ectodomain was correctly predicted. However, although six of the seven strands in the immunoglobulin-like domain were identified, the threading of the sequence was incorrect for the first four strands and was only exact within the last three of the seven strands characterizing the fold. This is the consequence of the fact that the immunoglobulin-like structure consists of strands from two different regions of the ectodomain; in particular, the first strand is not part of a continuous sequence with the other six strands. Table 1 documents the actual and predicted strands. Note, in particular, that the first of the seven β strands is localized near the beginning of the ectodomain (residues Glu88−Phe91) and approximately 85 amino acids separate it from the six remaining β strands of the fold. By contrast to the structure, the first β strand in the model is predicted to be located approximately on the sequence segment corresponding to the second β strand of the fold in the structure. This shift of one strand continues for the second and third strands of the model (see Table 1). The fourth strand of the model, close to the YYPYY conserved motif, corresponds to a loop in the structure. The threading of the last three strands of the fold, the fifth, sixth, and seventh, was correctly predicted. The seventh strand was predicted to exist previously on the basis of mutation work (*26*). It may affect the $\alpha-\beta$ assembly as observed in ref *26* by stabilizing the β ectodomain, since it is not in direct contact with the α subunit.

Overall, it is clear that the fold recognition servers identified the presence of an immunoglobulin-like fold within the ectodomain of the β subunit and pointed to the longest continuous

Table 1: Comparison of β Strands Found in the Structure of the β Subunit Ectodomain and Predicted by the Fold Recognition Servers

	Structure (shark beta1)	Model (human beta1)
Strand 1	88 EISF 91	~180-186
Strand 2	178 VAK 180	208 LPVQCTG 214
Strand 3	210 VLPLRCA 216	227 EYFG 230
Strand 4	229 IEYF 232	245 YGKLLQ 250
Strand 5	260 LLAIQF 265	256 PLLAVQF 262
Strand 6	274 LRIECKV 280	273 IECKAY 278
Strand 7	299 VKIEV 303	296 VKIEV 300

(C-terminal) fragment containing six of the seven β strands of the fold. The resemblance of the immunoglobulin-like fold, found mostly within the C-terminal lobe of the β subunit, to cell−cell adhesion molecules fits well with prior knowledge of the role in cell−cell adhesion of both β1 and β2 ectodomains. In addition, the modeling served to identify the region of the ectodomain that may be independently stable when expressed separately from the whole ectodomain. The expression, purification, and refolding of fragment 191−302, containing five strands, and CD experiments are consistent with this idea, as are the proteolytic digestion experiments. Expression of a somewhat longer segment (176−302), containing six of the seven strands of the fold, is also being planned.

We now discuss briefly possible functional implications of the observation that the C-terminal lobe of β resembles cell−cell adhesion or cell recognition molecules. According to the fold recognition results, one of the high-scoring structural templates is the V domain of nectin-like molecule 1 (necl-1), a cell−cell adhesion molecule, specifically expressed in neural tissue (*27*). necl-1 belongs to the necls family, sharing a common domain organization with nectins, which are Ca^{2+}-independent Ig-like cell adhesion molecules (CAMs). These proteins form homophilic cis dimers and homophilic or heterophilic trans dimers between neighboring cells involved in cell−cell adhesion (*28*). Nectin-based cell−cell adhesion is involved in many types of cell−cell junctions independently and cooperatively with other CAMs. necl-1 can interact with nectin-3 and nectin-1 at Junctia Adherina in neural cells. Nectin-1 and nectin-3 are ubiquitously expressed in various tissues and are important for the formation of AJ's in epithelial cells (*29*). The β ectodomain could be similarly involved in homodimerization with β subunits, and/or heterodimerization with other molecules such as nectins, at the sites of AJ. This hypothesis of an interaction with nectin(s) is compatible with knowledge of common localization of nectins, E-cadherin, and the Na,K-ATPase at AJ. In particular, nectins and Na,K-ATPase are found in cell−cell contact sites from the initial stages of formation (*5*, *28*). necl-1 is the only member of the necls and nectin families with partially known structure (*30*), but it is conceivable that the V domains (the outermost domains) of other nectin-like and nectin molecules have a similar structure. As a test of the hypothesis about possible interactions with Na,K-ATPase in AJ, the sequence of the V domain of nectin-3, with unknown structure, was submitted to the 3D-Jury meta-server. Indeed, several of the highest-scoring predicted templates for nectin-3 (Jscore $\leq$ 82) were the same as found for β1: 1neu (neural membrane adhesion molecule P0), 2icc (CRIg), 2pnd (CRIg),

1py9 (autoantigen in multiple sclerosis), and 1pko (myelin oligodendrocyte glycoprotein).

The segments of the β subunit oriented to the extracellular medium, and not in direct contact with the α subunit, are candidates for interactions with other proteins. It is known that much of the ectodomain is not absolutely essential for assembly of β with α and trafficking to the plasma membrane (*31*), but it is also known that mutations within the ectodomain preclude formation of functional pumps, implying that an intact ectodomain is necessary for function (*26*, *32*). The structure of shark rectal gland Na,K-ATPase shows that there are four segments of the ectodomain in direct contact with the extracellular loops of α, primarily L7/8, including segments of residues Leu62−Lys86, Lys180−Ile185, Tyr247−Lys250, and Lys290−Phe293 (*16*).[2] Much of the surface of the ectodomain, including the majority of the immunoglobulin-like structure, is not in direct contact with the α subunit and could interact with other proteins. As an example, the segment between the second and third strand of the immunogobulin-like fold of β1, corresponding to the loop containing the subtilisin cleavage site (see Figure 8), is an insertion in β1 relative to all the other isoforms (see Figure 1). This loop is exposed to the extracellular space, making it a candidate for β1- selective interactions with proteins in AJ, where β1 is localized, but not other β isoforms. An antibody which recognizes a sequence in this loop has already been shown to interfere with adhesion of MDCK cells (*5*).

As mentioned in the introductory section, β2 (but not β1) has long been known to mediate cell adhesion between neurons and astrocytes in rat brain (*10*, *33*). Thus, it is possible that the β2 ectodomain undergoes interaction with cell adhesion molecules that are expressed in the nervous system, for example, necl-1 (*27*), which is one of the high-scoring template structures. Since β2 lacks the loop unique to the β1 isoform, one could speculate that other segment of β2 is responsible for interactions between astrocytes and neurons. In cases where β2 is expressed on the apical side of some epithelia (*34*), it may be involved in protein−protein interactions on the same cell, i.e., cis interactions.

In the case of the gastric H,K-ATPase, there is no specific prior information about a protein−protein interaction function of the β subunit. A new structure of the H,K-ATPase at 6.5 Å resolution, based on cryoelectron microscopy, reveals a modular organization of the β subunit ectodomain, including a lobe that appears to be relatively independent of the α subunit (*18*). A fit of the model of the C-terminal lobe (see Figure 3C) into the electron density map shows that the dimensions of the model fit rather well with this relatively independent lobe of the electron density map (not shown). Thus, it is reasonable to identify this density with the C-terminal lobe of βHK. Because the predicted fold of this domain is so common to cell adhesion and cell recognition molecules, and the lobe does not appear to be in direct contact with the α subunit, it is possible that this domain of βHK is also involved in protein−protein interactions. Since βHK at the apical surface of the gastric mucosa should not act as a cell−cell adhesion molecule, it is possible that it is involved in cis interactions on the same cell.

Although it is not strictly relevant to the structural predictions in this paper, it is worth pointing out that the human β1 ectodomain contains an RGD motif in a loop facing the extracellular space. This motif might mediate an interaction with an RGD motif binding integrin $\alpha v\beta 3$ found in AJ (*28*). Interestingly, β2 and β3 isoforms that do not localize at AJ do not have the RGD motif. However, the RGD sequence is not fully conserved in β1. Most species have either an RGD or RGE [that was also shown to bind integrins (*35*)] sequence, but it is RGP in chicken and *Torpedo*.

[2]The Leu62−Lys86 and Lys180−Ile185 sequences are close to two sequences inferred to contain residues in contact with the α subunit by Cu-mediated oxidative cleavage (*36*).

CONCLUSIONS

The major conclusion of this paper is that there is a structural analogy of the C-terminal lobe of the β ectodomain with cell−cell adhesion molecules. The purified, refolded C-terminal part of the β subunits may, therefore, provide an experimental tool for identification of proteins interacting with β in the extracellular space, including a search for specific regions involved in protein−protein interactions, and study of its physiological role in cellular adhesion.

ACKNOWLEDGMENT

We are grateful to Prof. David Stokes (New York University, New York, NY) and Dr. Kazihuro Abe (Kyoto University, Kyoto, Japan) for providing us with electron density maps of renal Na,K-ATPase and gastric H,K-ATPase, respectively. We are grateful to Prof. Chikashi Toyoshima, Tokyo University, for helpful comments on this work.

REFERENCES

1. Geering, K. (2001) The functional role of β subunits in oligomeric P-type ATPases. *J. Bioenerg. Biomembr. 33*, 425–438.
2. Geering, K. (2008) Functional roles of Na,K-ATPase subunits. *Curr. Opin. Nephrol. Hypertens. 17*, 526–532.
3. Rajasekaran, S. A., Barwe, S. P., and Rajasekaran, A. K. (2005) Multiple functions of Na,K-ATPase in epithelial cells. *Semin. Nephrol. 25*, 328–334.
4. Rajasekaran, S. A., Palmer, L. G., Quan, K., Harper, J. F., Ball, W. J. Jr., Bander, N. H., Peralta Soler, A., and Rajasekaran, A. K. (2001) Na,K-ATPase β-subunit is required for epithelial polarization, suppression of invasion, and cell motility. *Mol. Biol. Cell 12*, 279–295.
5. Vagin, O., Tokhtaeva, E., and Sachs, G. (2006) The role of the β1 subunit of the Na,K-ATPase and its glycosylation in cell-cell adhesion. *J. Biol. Chem. 281*, 39573–39587.
6. Barwe, S. P., Anilkumar, G., Moon, S. Y., Zheng, Y., Whitelegge, J. P., Rajasekaran, S. A., and Rajasekaran, A. K. (2005) Novel role for Na,K-ATPase in phosphatidylinositol 3-kinase signaling and suppression of cell motility. *Mol. Biol. Cell 16*, 1082–1094.
7. Kitamura, N., Ikekita, M., Sato, T., Akimoto, Y., Hatanaka, Y., Kawakami, H., Inomata, M., and Furukawa, K. (2005) Mouse Na^+/K^+-ATPase β1-subunit has a K^+-dependent cell adhesion activity for β-GlcNAc-terminating glycans. *Proc. Natl. Acad. Sci. U.S.A. 102*, 2796–2801.
8. Vagin, O., Tokhtaeva, E., Yakubov, I., Shevchenko, E., and Sachs, G. (2008) Inverse correlation between the extent of N-glycan branching and intercellular adhesion in epithelia. Contribution of the Na,K-ATPase β1 subunit. *J. Biol. Chem. 283*, 2192–2202.
9. Shoshani, L., Contreras, R. G., Roldan, M. L., Moreno, J., Lazaro, A., Balda, M. S., Matter, K., and Cereijido, M. (2005) The polarized expression of Na^+,K^+-ATPase in epithelia depends on the association between β-subunits located in neighboring cells. *Mol. Biol. Cell 16*, 1071–1081.
10. Gloor, S., Antonicek, H., Sweadner, K. J., Pagliusi, S., Frank, R., Moos, M., and Schachner, M. (1990) The adhesion molecule on glia (AMOG) is a homologue of the β subunit of the Na,K-ATPase. *J. Cell Biol. 110*, 165–174.
11. Schmalzing, G., Ruhl, K., and Gloor, S. M. (1997) Isoform-specific interactions of Na,K-ATPase subunits are mediated via extracellular domains and carbohydrates. *Proc. Natl. Acad. Sci. U.S.A. 94*, 1136–1141.
12. Colonna, T. E., Huynh, L., and Fambrough, D. M. (1997) Subunit interactions in the Na,K-ATPase explored with the yeast two-hybrid system. *J. Biol. Chem. 272*, 12366–12372.
13. Morth, J. P., Pedersen, B. P., Toustrup-Jensen, M. S., Sorensen, T. L., Petersen, J., Andersen, J. P., Vilsen, B., and Nissen, P. (2007)

Crystal structure of the sodium-potassium pump. *Nature 450*, 1043–1049.
14. Ginalski, K., Elofsson, A., Fischer, D., and Rychlewski, L. (2003) 3D-Jury: A simple approach to improve protein structure predictions. *Bioinformatics 19*, 1015–1018.
15. Fischer, D. (2006) Servers for protein structure prediction. *Curr. Opin. Struct. Biol. 16*, 178–182.
16. Shinoda, T., Ogawa, H., Cornelius, F., and Toyoshima, C. (2009) Crystal structure of the sodium-potassium pump at 2.4 Å resolution. *Nature 459*, 446–450.
17. Rice, W. J., Young, H. S., Martin, D. W., Sachs, J. R., and Stokes, D. L. (2001) Structure of Na^+,K^+-ATPase at 11-Å resolution: Comparison with Ca^{2+}-ATPase in E1 and E2 states. *Biophys. J. 80*, 2187–2197.
18. Abe, K., Tani, K., Nishizawa, T., and Fujiyoshi, Y. (2009) Inter-subunit interaction of gastric H^+,K^+-ATPase prevents reverse reaction of the transport cycle. *EMBO J. 28*, 1637–1643.
19. Peleg, Y., and Unger, T. (2008) Application of high-throughput methodologies to the expression of recombinant proteins in *E. coli*. *Methods Mol. Biol. 426*, 197–208.
20. Brumfeld, V., and Werber, M. M. (1993) Studies on fibronectin and its domains. II. Secondary structure and spatial configuration of fibronectin and of its domains. *Arch. Biochem. Biophys. 302*, 134–143.
21. Perez-Iratxeta, C., and Andrade-Navarro, M. A. (2008) K2D2: Estimation of protein secondary structure from circular dichroism spectra. *BMC Struct. Biol. 8*, 25.
22. Haviv, H., Cohen, E., Lifshitz, Y., Tal, D. M., Goldshleger, R., and Karlish, S. J. (2007) Stabilization of Na^+,K^+-ATPase Purified from *Pichia pastoris* Membranes by Specific Interactions with Lipids. *Biochemistry 46*, 12855–12867.
23. Fischer, D., Pas, J., and Rychlewski, L. (2004) The PDB-Preview database: A repository of in-silico models of "on-hold" PDB entries. *Bioinformatics 20*, 2482–2484.
24. Fuzesi, M., Gottschalk, K. E., Lindzen, M., Shainskaya, A., Kuster, B., Garty, H., and Karlish, S. J. (2005) Covalent cross-links between the γ subunit (FXYD2) and α and β subunits of Na,K-ATPase: Modeling the α-γ interaction. *J. Biol. Chem. 280*, 18291–18301.
25. Holm, L., and Sander, C. (1993) Protein structure comparison by alignment of distance matrices. *J. Mol. Biol. 233*, 123–138.
26. Beggah, A. T., Beguin, P., Jaunin, P., Peitsch, M. C., and Geering, K. (1993) Hydrophobic C-terminal amino acids in the β-subunit are involved in assembly with the α-subunit of Na,K-ATPase. *Biochemistry 32*, 14117–14124.
27. Kakunaga, S., Ikeda, W., Itoh, S., Deguchi-Tawarada, M., Ohtsuka, T., Mizoguchi, A., and Takai, Y. (2005) Nectin-like molecule-1/TSLL1/SynCAM3: A neural tissue-specific immunoglobulin-like cell-cell adhesion molecule localizing at non-junctional contact sites of presynaptic nerve terminals, axons and glia cell processes. *J. Cell Sci. 118*, 1267–1277.
28. Sakisaka, T., Ikeda, W., Ogita, H., Fujita, N., and Takai, Y. (2007) The roles of nectins in cell adhesions: Cooperation with other cell adhesion molecules and growth factor receptors. *Curr. Opin. Cell Biol. 19*, 593–602.
29. Takai, Y., Irie, K., Shimizu, K., Sakisaka, T., and Ikeda, W. (2003) Nectins and nectin-like molecules: Roles in cell adhesion, migration, and polarization. *Cancer Sci. 94*, 655–667.
30. Dong, X., Xu, F., Gong, Y., Gao, J., Lin, P., Chen, T., Peng, Y., Qiang, B., Yuan, J., Peng, X., and Rao, Z. (2006) Crystal structure of the V domain of human Nectin-like molecule-1/Syncam3/Tsll1/Igsf4b, a neural tissue-specific immunoglobulin-like cell-cell adhesion molecule. *J. Biol. Chem. 281*, 10610–10617.
31. Laughery, M. D., Todd, M. L., and Kaplan, J. H. (2003) Mutational analysis of α-β subunit interactions in the delivery of Na,K-ATPase heterodimers to the plasma membrane. *J. Biol. Chem. 278*, 34794–34803.
32. Geering, K., Jaunin, P., Jaisser, F., Merillat, A. M., Horisberger, J. D., Mathews, P. M., Lemas, V., Fambrough, D. M., and Rossier, B. C. (1993) Mutation of a conserved proline residue in the β-subunit ectodomain prevents Na^+-K^+-ATPase oligomerization. *Am. J. Physiol. 265*, C1169–C1174.
33. Muller-Husmann, G., Gloor, S., and Schachner, M. (1993) Functional characterization of β isoforms of murine Na,K-ATPase. The adhesion molecule on glia (AMOG/β 2), but not β 1, promotes neurite outgrowth. *J. Biol. Chem. 268*, 26260–26267.
34. Vagin, O., Turdikulova, S., and Tokhtaeva, E. (2007) Polarized membrane distribution of potassium-dependent ion pumps in epithelial cells: Different roles of the N-glycans of their β subunits. *Cell Biochem. Biophys. 47*, 376–391.
35. Humtsoe, J. O., Bowling, R. A.Jr., Feng, S., and Wary, K. K. (2005) Murine lipid phosphate phosphohydrolase-3 acts as a cell-associated integrin ligand. *Biochem. Biophys. Res. Commun. 335*, 906–919.
36. Bar Shimon, M. B., Goldshleger, R., and Karlish, S. J. (1998) Specific Cu^{2+}-catalyzed oxidative cleavage of Na,K-ATPase at the extracellular surface. *J. Biol. Chem. 273*, 34190–34195.